Electronic Supplementary Material (ESI) for Soft Matter.

Supplemental Material for When droplets become stars: charged dielectric droplets beyond the Rayleigh limit

Myong In Oh,[1] Anatoly Malevanets,[2] Maxim Paliy,[1] Daan Frenkel,[3] and Styliani Consta[1,3]

[1] *Department of Chemistry, The University of Western Ontario, London N6A 5B7, Ontario, Canada*
[2] *Department of Electrical and Computer Engineering, The University of University of Western Ontario, London N6A 5B9, Ontario, Canada*
[3] *Department of Chemistry, University of Cambridge, Lensfield Road, Cambridge, CB2 1EW, United Kingdom*

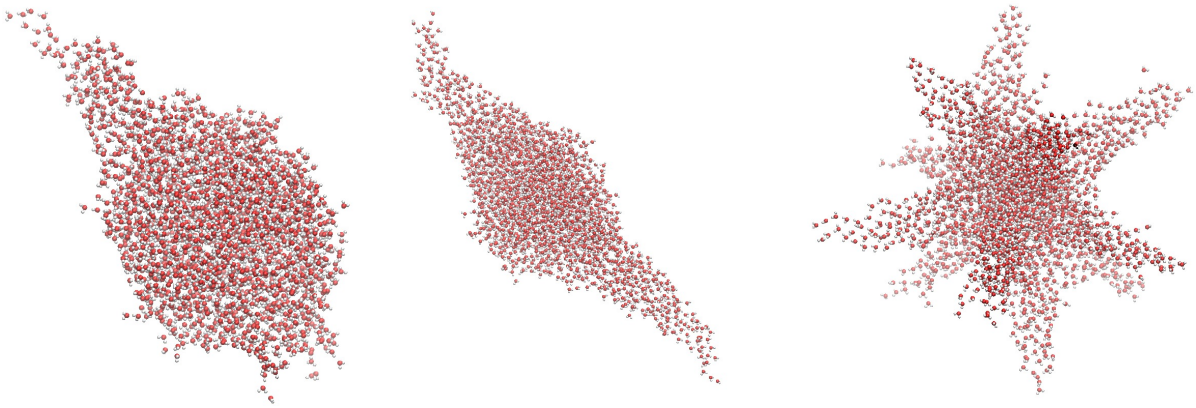

(a) $Q = 14$ (1 ray) (b) $Q = 15$ (2 rays) (c) $Q = 40$ (12 rays)

FIG. S1: Typical snapshots of charged aqueous droplets at $T = 300$ K. All the droplets are composed of 2148 TIP3P-H_2O molecules and have an embedded model spherical ion. The charge at the instability limit for these droplets is $Q_R \approx 13.3$ and $Q_I \approx 13.9$.

S1. SIMULATION DETAILS FOR A CHARGED C_{60}-DROPLET SYSTEM

A charged buckyball (C_{60}) is selected as a representative macroion. Charged fullerenes have been obtained in experiments by, for example, functionalization[1], fullerides[2–5], and protonation in superacids[6]. The C_{60} was placed in a droplet of SPC/E water [7, 8]. The OPLS-AA force field model (which includes long-range electrostatic Coulomb terms and short-range Lennard-Jones (LJ) terms) was employed to represent the energetics of all the species, including SPC/E water [7, 8]. Molecular Dynamics (MD) simulations of the droplets with the C_{60} were carried out using the GROMACS[9] package version 4.5.5. To prevent solvent escape, droplets with a radius of up to ≈ 3.7 nm containing up to ≈ 2500 molecules of solvent an spherical cavity of 20 nm in diameter, made of Lennard-Jones atoms uniformly distributed on a sphere. Such a set-up effectively fixes the external pressure of the solvent at the vapour value for a droplet of the given size. After the preliminary energy minimization and equilibration at constant temperature $T =$ 300 K with a neutral buckyball, the resulting configurations were used to initialize simulations with charged buckyballs. Simulations for aqueous droplets were performed at every integer charge from $|Q| = 16$ e to $|Q| = 36$ e (where e is the elementary positive charge) for both positively and negatively charged buckyballs. Electrostatics was treated explicitly. Typically, we performed constant temperature simulations of up to 10 ns duration. Thermostating was achieved by the 'quick-and-dirty' velocity rescaling. The electrostatic potentials were calculated using the "volmap" function of VMD, using the "coumlombmsm" method.

S2. SHAPES OF AQUEOUS DROPLETS WITH AN EMBEDDED SPHERICAL MODEL MACROION

The shapes of aqueous droplets with $Q = 14, 15, 40$ are shown in Fig. S1.

For the case of Q=15 (Fig. S1b), the least stable mode is the $l = 2$. For $Q = 40$ (Fig. S1c), the modes with $l = 16, 17, 18$ are the least stable.

a. Fastest growing mode analysis For Q=15 (Fig. S1b) the fastest growing mode (estimated using Eq. 8 in the main text) is $l = 1$, for $Q = 40$ (Fig. S1c) are those with $l = 5, 6, 7$. For $Q = 22$ (Fig. 2 in the main text) the fastest growing mode is the $l = 3$. Simulations show that the final droplets have a predominant $l = 3$ character (see Fig. 3 in the main text). For $Q = 27$ (Fig. 2 in the main text) the fastest growing mode is $l = 4$. The simulations show that the droplet has six points, and it has a predominant l = 4 character (Fig. 3 in the main text). For Q =32 (Fig. 2 in main text) the fastest growing modes are $l = 4, 5$. As Fig. 3 (in the main text) shows, the final droplet has a strong $l = 4$ and 5 character. And finally, for $Q = 36$ (Fig. 2 in the main text) the fastest growing modes are $l = 5, 6$. Figure 3 in the main text shows that the final droplet shape is dominated by $l = 5$ modes.

S3. EXAMPLES OF FASTEST GROWING MODE AND LEAST STABLE MODE

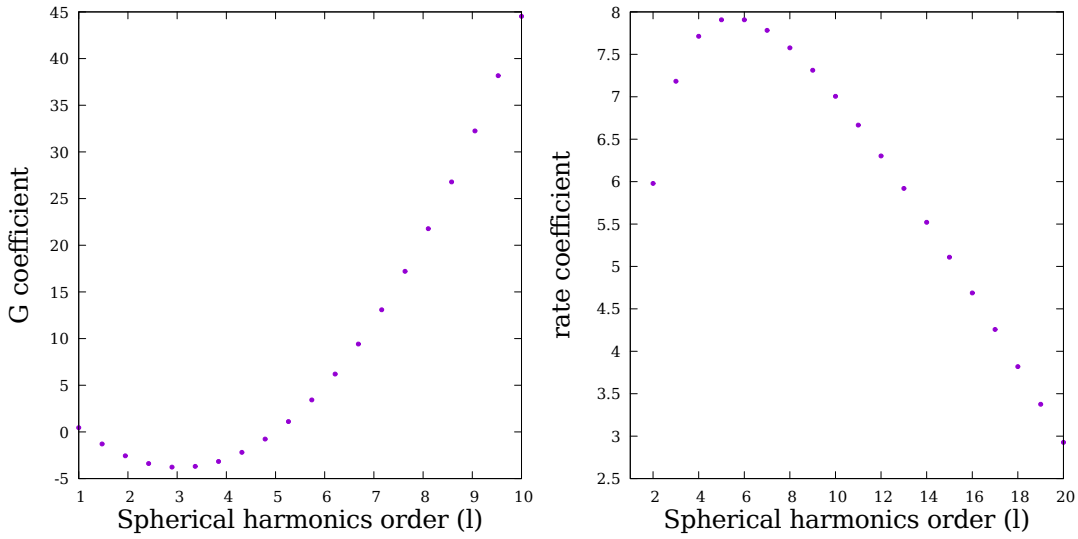

(a) (b)

FIG. S2: (a) $G(l, X, \epsilon^I)$ vs the order of the spherical harmonics for $Q = 18$. (b) $-C_l = -G(l, X, \epsilon^I)\frac{l(2l+1)}{2(l-1)(2l^2+4l+3)}$ vs the order of the spherical harmonics for $Q = 36$.

S4. RESULTS FOR A CHARGED C_{60}-DROPLET SYSTEM

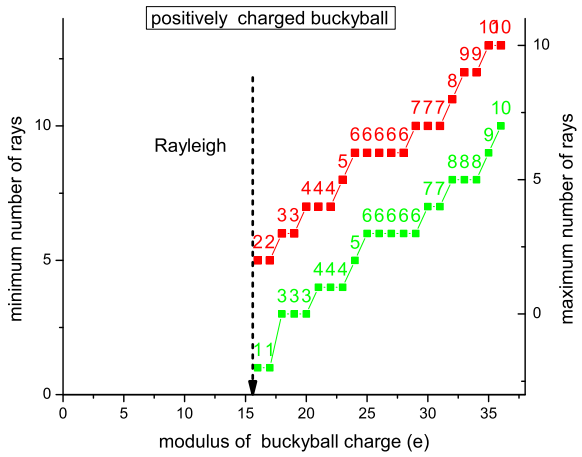

(a) Positive

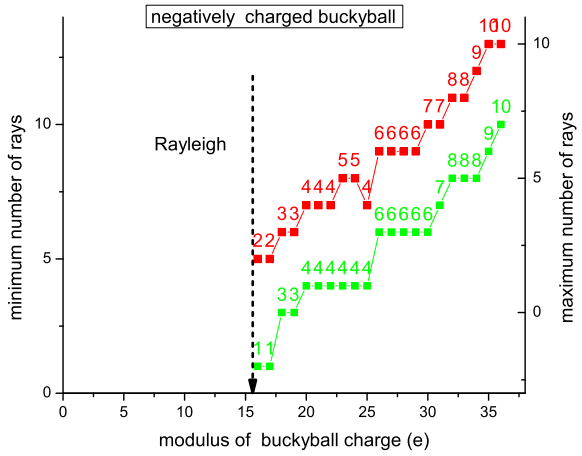

(b) Negative

FIG. S3: Minimum (green squares) and maximum (red squares) number of points in the aqueous droplets versus Q for (a) positive and (b) negative buckyball charge. The lines connecting the squares are drawn as a guide to the eye. For clarity purpose, the maximum number of rays (measured in the right axis) has been shifted relative to the minimum number of rays (measured in the left axis). The data were collected after 1 ns equilibration time. The instability limit for aqueous charged droplets at $Q_I = 15.5$ is marked with a dashed vertical line.

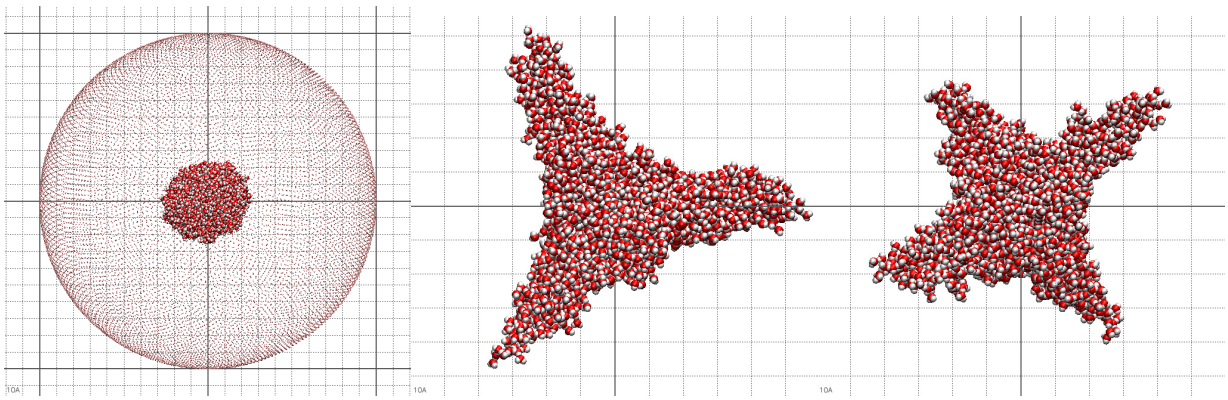

(a) $Q = 0$ (b) $Q = 18$ (3 rays) (c) $Q = 24$ (4 rays)

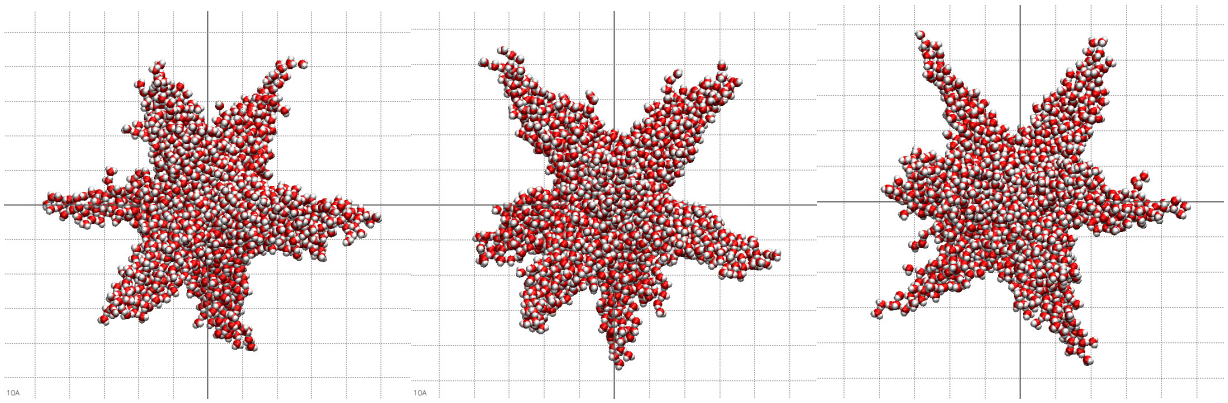

(d) $Q = 28$ (6 rays) (e) $Q = 32$ (8 rays) (f) $Q = 36$ (10 rays)

FIG. S4: Typical snapshots of (a) an uncharged aqueous droplet, and charged aqueous droplets (b)-(f) . The charged droplet were prepared after 10 ns of simulation at $T = 300$ K starting from configuration (a). All the droplets are composed of 2148 H_2O molecules and have an embedded buckyball inside. The charge of the buckyball is varied. The charge at the instability limit for these systems is $Q_I \approx 15.5$. To indicate the scale of the snapshots, we show a background grid with a lattice spacing of 1 nm.

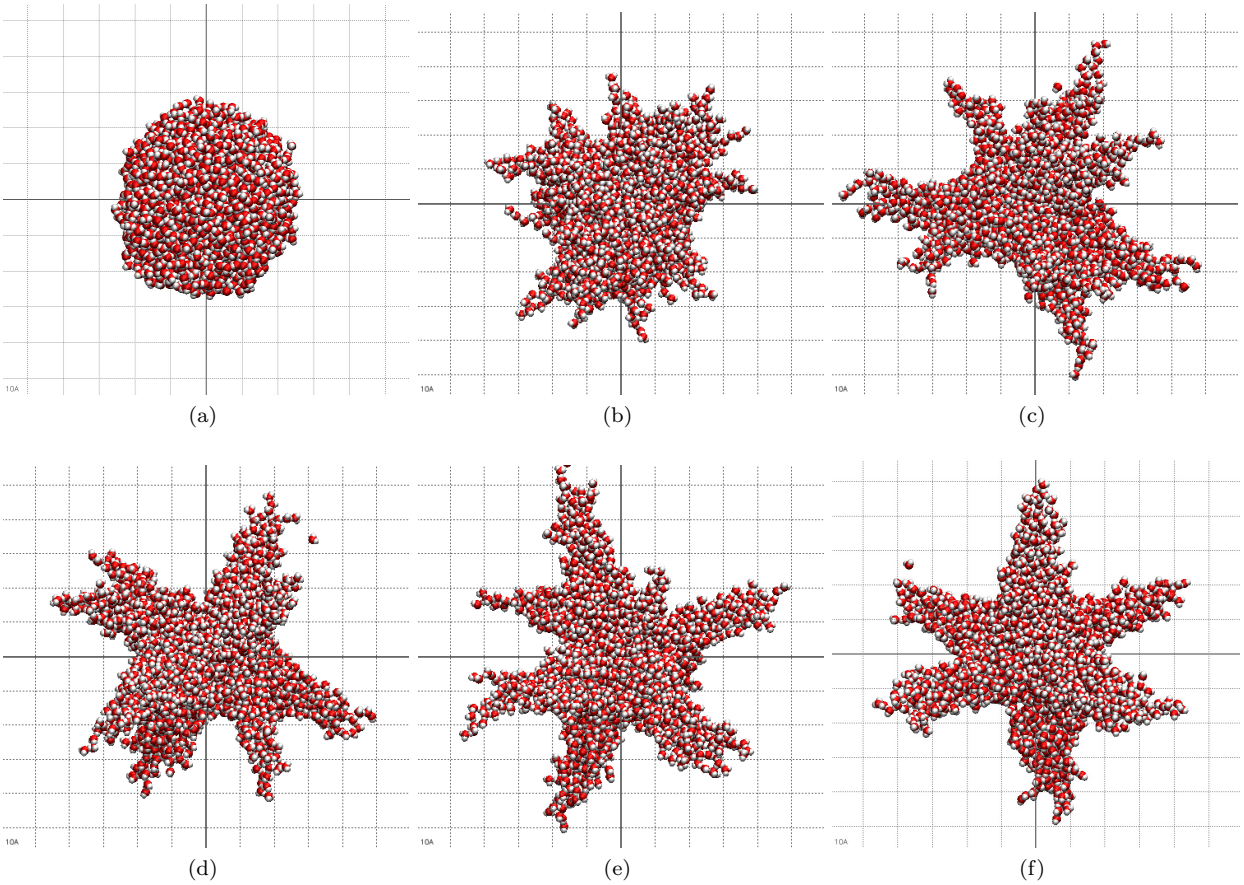

FIG. S5: Early stages of time evolution of an aqueous droplet composed of 2148 molecules and charged to $Q = 28$ at $T = 300$ K: (a) initial configuration $t = 0$ ns; (b) $t = 0.020$ ns, more than twenty small rays emerge from the surface; (c) $t = 0.060$ ns, more than 12 rays are visible; (d) $t = 0.200$ ns, 8 rays are visible; (e) $t = 0.400$ ns, 7 rays are visible; (f) $t = 1.0$ ns, final configuration of 6 rays, that is stable up to $t = 10.0$ ns. The Rayleigh limit charge is $Q_R = 15.5$. The grid size is 1 nm.

S5. "POWER SPECTRUM" OF THE STAR SHAPES

In practice, we determine the spherical harmonics power spectrum from analysis of the atom distribution in an angle-dependent cone

$$r^2(\theta,\phi) = \frac{5}{3}\frac{1}{N_{\Delta\theta,\Delta\phi}} \sum_{i\in\Delta\theta,\Delta\phi} (\vec{r}_i - \vec{r}_{centre})^2, \tag{S1}$$

where $N_{\Delta\theta,\Delta\phi}$ is the number of atoms in a solid angle $(\Delta\theta, \Delta\phi)$ around θ, ϕ. Although more sophisticated schemes exist [10], we opted for simplicity and computed $r^2(\theta,\phi)$ on a regular grid: we took 36 $\cos\theta_j$ points, uniformly distributed between $\cos\theta = 1$ and $\cos\theta = -1$, and 72 uniformly distributed ϕ_k points in the azimuthal direction.

From 5-ns long trajectories we selected 200 sample time points, calculated the power spectrum Eq. 7a (main text) for each point, and averaged spectra over the trajectories. The averaged power spectra for five representative "star-droplets" covering the entire range of charges studied above Rayleigh limit $18 < Q < 36$, from 3-points to 10-points stars, are shown in Fig. 3 (in the main text). The spherical harmonics order cut-off $l_{\max} = 15$ was sufficient to obtain all the salient features of the star shape. We also note here that our simple shape description Eq. S1 gives a reliable representation of the droplet shape, as is evident from Fig. S6 and Fig. S7, where we compare the spherical harmonics spectra and reconstructed shapes obtained from both the Eq. S1 and the full molecular surface represented by an iso-surface of the atomic density.

S6. RECONSTRUCTION OF THE SHAPES

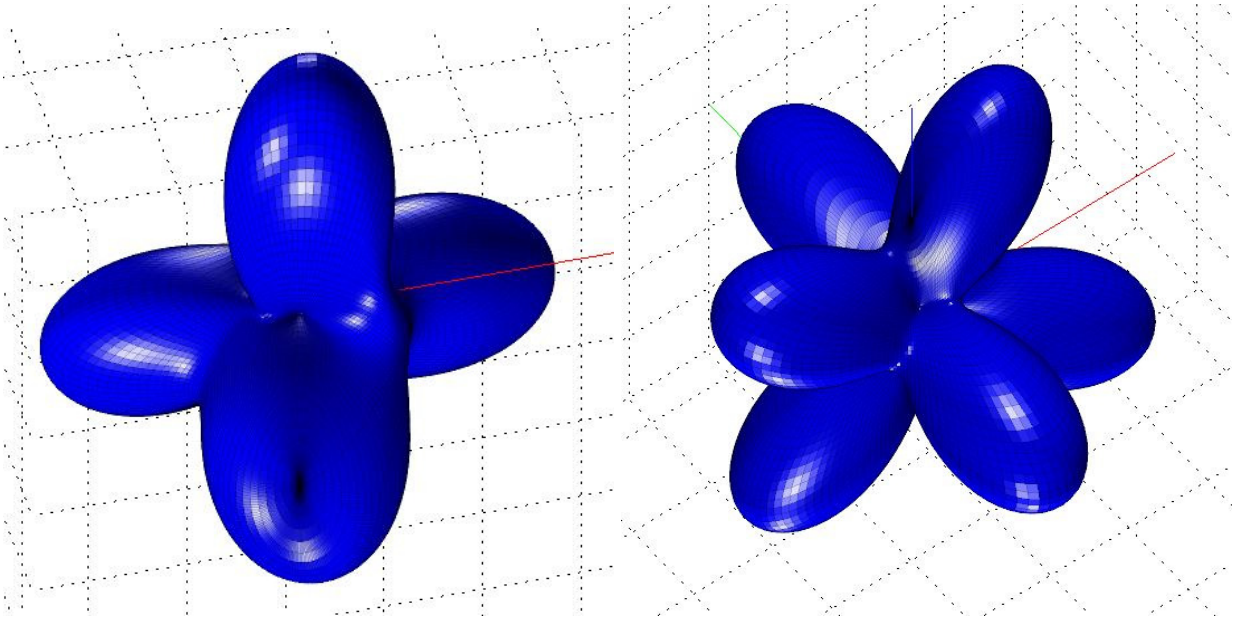

FIG. S6: Spherical harmonics reconstruction of the shapes of 4-rays tetrahedral star (left) and 6-rays star (right) depicted in the Fig. 1 (c) and (d) in the main text, respectively. The maximum order of spherical harmonics used is $l = 5$.

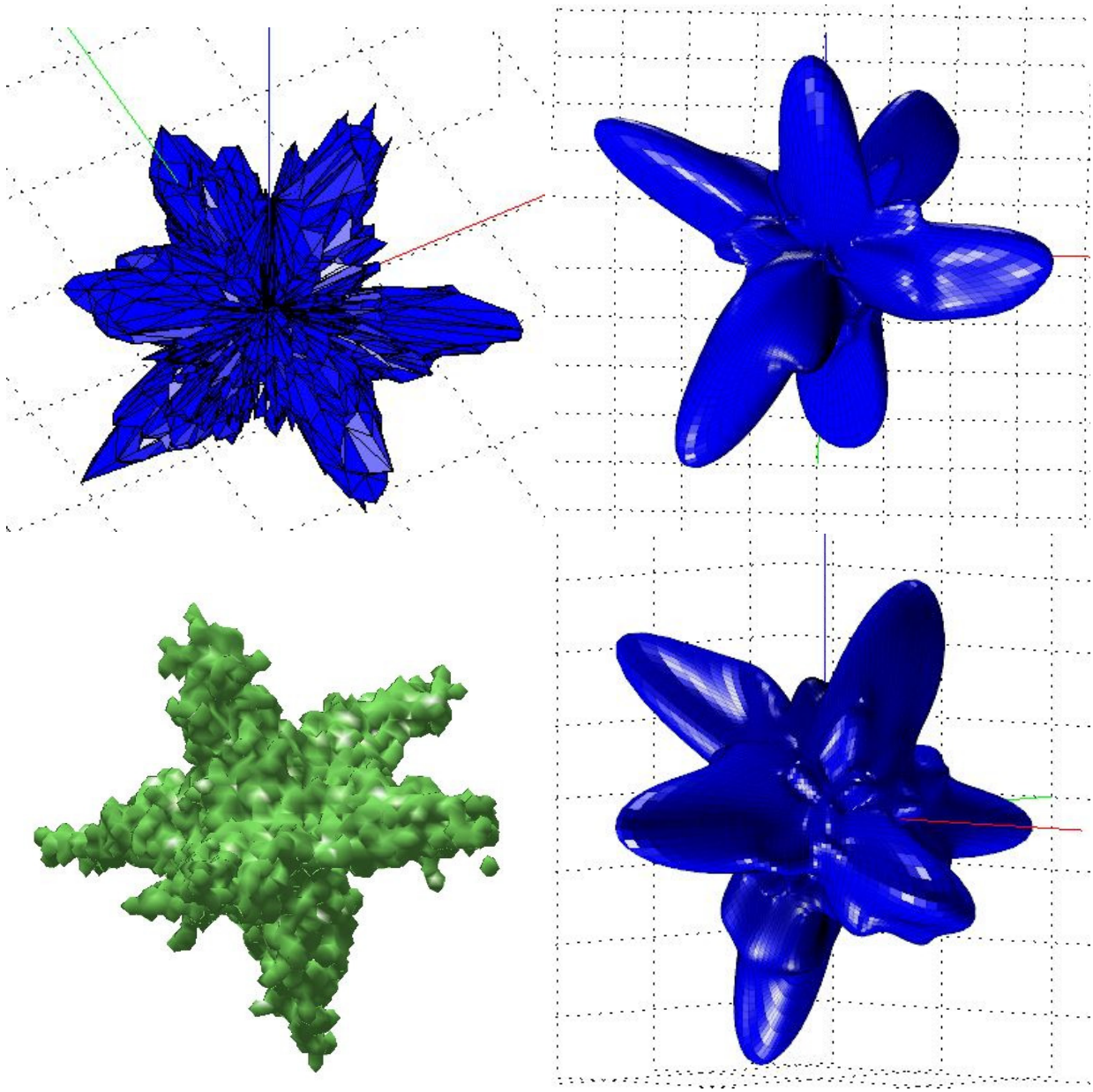

FIG. S7: Top: angle-dependent radius of gyration ($R_g(\theta, \phi)$), and its spherical harmonics reconstruction using first $l_{max} = 15$ harmonics. Bottom: isosurface of the atomic density at the value of 0.1 and its its spherical harmonics reconstruction using first $l_{max} = 15$ harmonics. The charged water droplet is the same as shown in the Fig. 1 of the main text at $Q_R = +28$, 6-rays star.

S7. CURVATURE CORRECTIONS

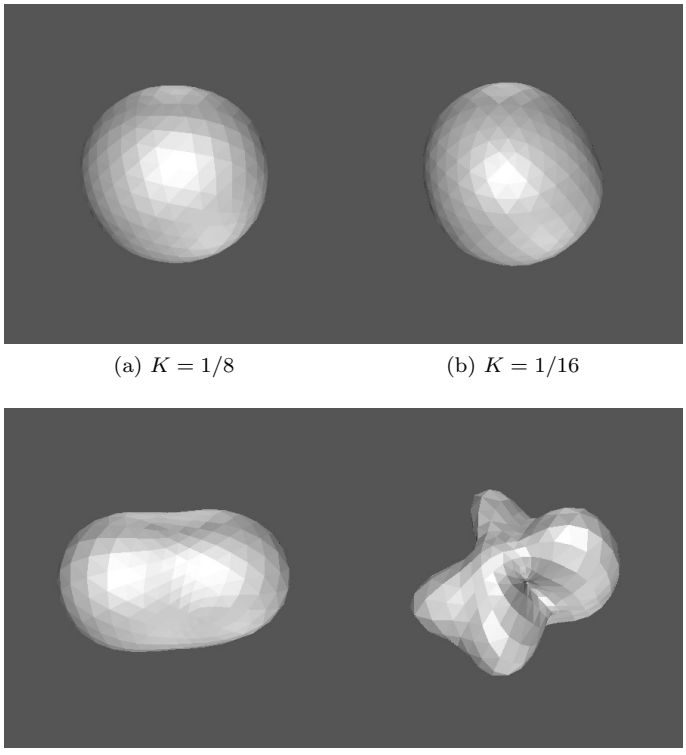

(a) $K = 1/8$ (b) $K = 1/16$

(c) $K = 1/32$ (d) $K = 1/2048$

FIG. S8: Final states of Monte Carlo runs using the Helfrich correction.

[1] N. O. Mchedlov-Petrossyan, Chem. Rev. **113**, 5149 (2013).
[2] C. A. Howard and N. T. Skipper, J. Phys. Chem. B **113**, 3324 (2009).
[3] A. Penicaud, P. Poulin, A. Derre, E. Anglaret, and P. Petit, J. Am. Chem. Soc. **127**, 8 (2004).
[4] D. Voiry, C. Drummond, and A. Pénicaud, Soft Matter **7**, 7998 (2011).
[5] S. Fogden, C. A. Howard, R. K. Heenan, N. T. Skipper, and M. S. P. Shaffer, ACS Nano **6**, 54 (2011).
[6] S. Ramesh, L. M. Ericson, V. A. Davis, R. K. Saini, C. Kittrell, M. Pasquali, W. E. Billups, W. W. Adams, R. H. Hauge, and R. E. Smalley, J. Phys. Chem. B **108**, 8794 (2004).
[7] W. L. Jorgensen and D. L. Severance, J. Am. Chem. Soc. **112**, 4768 (1990).
[8] W. L. Jorgensen and J. Tirado-Rives, Proc. Natl. Acad. Sci. U.S.A. **102**, 6665 (2005).
[9] B. Hess, C. Kutzner, D. van der Spoel, and E. Lindahl, J. Chem. Theory Comput. **4**, 435 (2008).
[10] V. Lebedev and D. Laikov, Doklady. Mathematics **59**, 477 (1999).